Electronic Supporting Information (ESI)

Built-in Electric Field Induced Interfacial Charge Distributions of $Ni_2P/NiSe_2$ Heterojunction for Urea-Assisted Hydrogen Evolution Reaction

Yiqiang Sun[#,a], Wenwen Cao[#,a], Xuening Ge [a], Xiaodong Yang [a], Yong Wang[b], Yuan Xu[b], Bo Ouyang[,c], Qi Shen[*,a], Cuncheng Li[*,a]*

Prof. Y. Q. Sun, Dr. W. W. Cao, X. N. Ge, X. D. Yang, C. C. Wang, Q. Shen, Prof. C. C. Li

School of Chemistry and Chemical Engineering, University of Jinan, Jinan, 250055, P. R. China

Dr. Y Wang, Prof. Y. Xu

Hongyuan Waterproof Technology Group Co., Ltd, 250055, P. R. China

Dr. Bo Ouyang

MIIT Key Laboratory of Semiconductor Microstructure and Quantum Sensing, Nanjing University of Science and Technology, Nanjing 210094, P. R. China.

E-mail: ouyangboyi@njust.edu.cn; chm_shenq@ujn.edu.cn; chm_licc@ujn.edu.cn

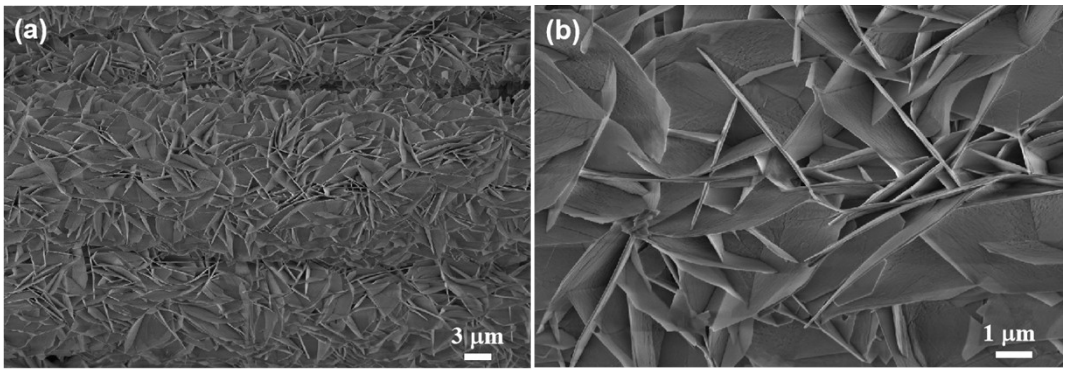

Fig. S1 (a) Low-magnification SEM image and (b) High-magnification SEM image of $Ni(OH)_2$/CFC nanosheet arrays precursor.

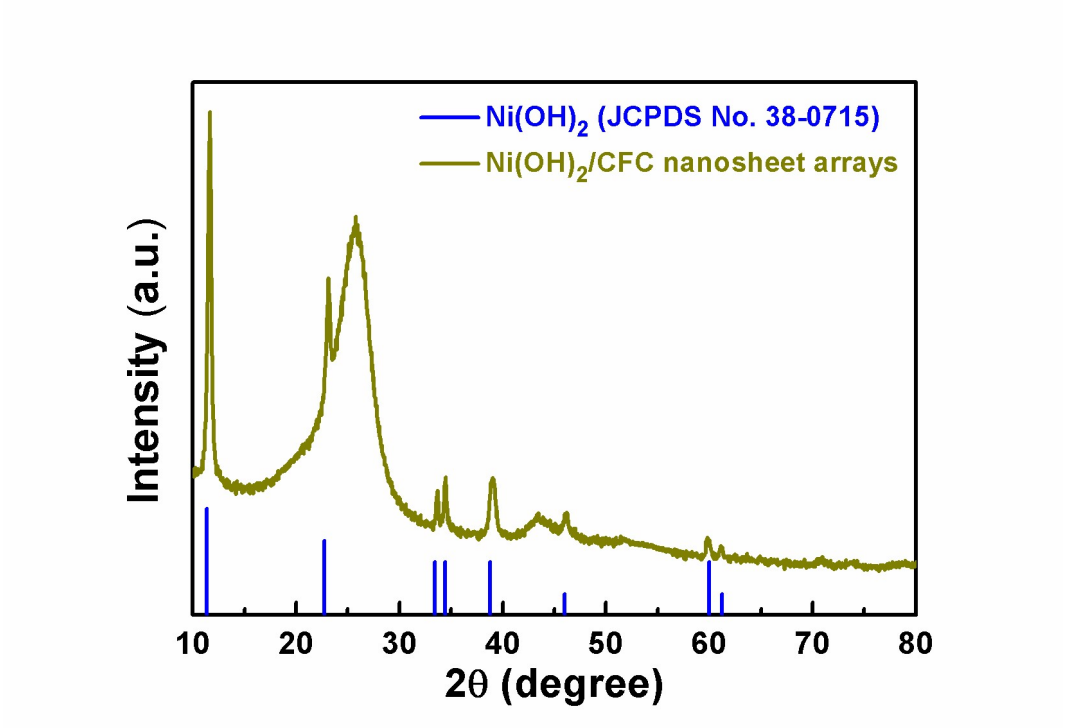

Fig. S2 XRD pattern of $Ni(OH)_2$/CFC nanosheet arrays precursor.

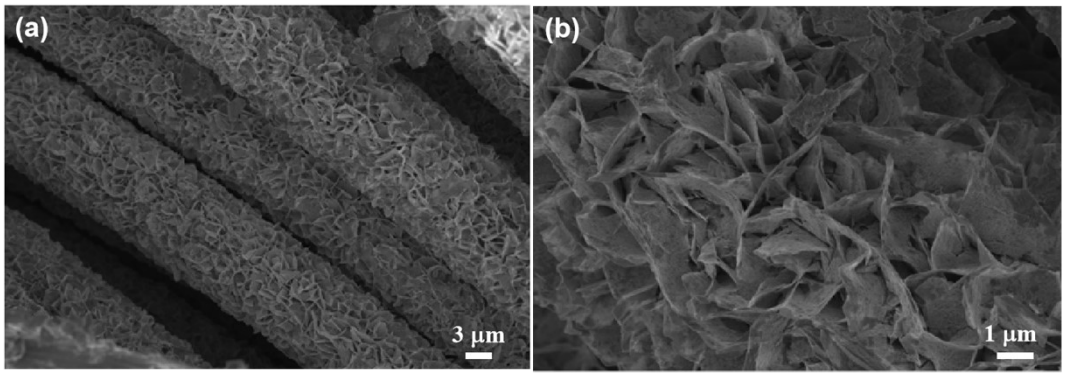

Fig. S3 (a) Low-magnification SEM image and (b) High-magnification SEM image of Ni_2P/CFC nanosheet arrays.

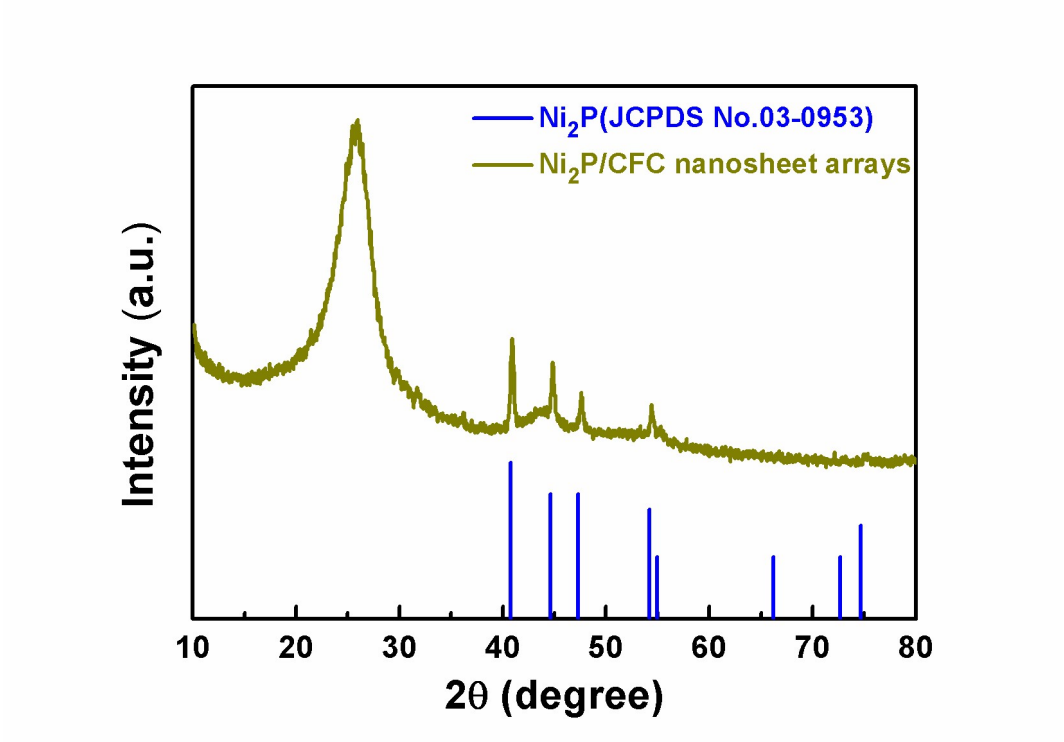

Fig. S4 XRD pattern of Ni_2P/CFC nanosheet arrays.

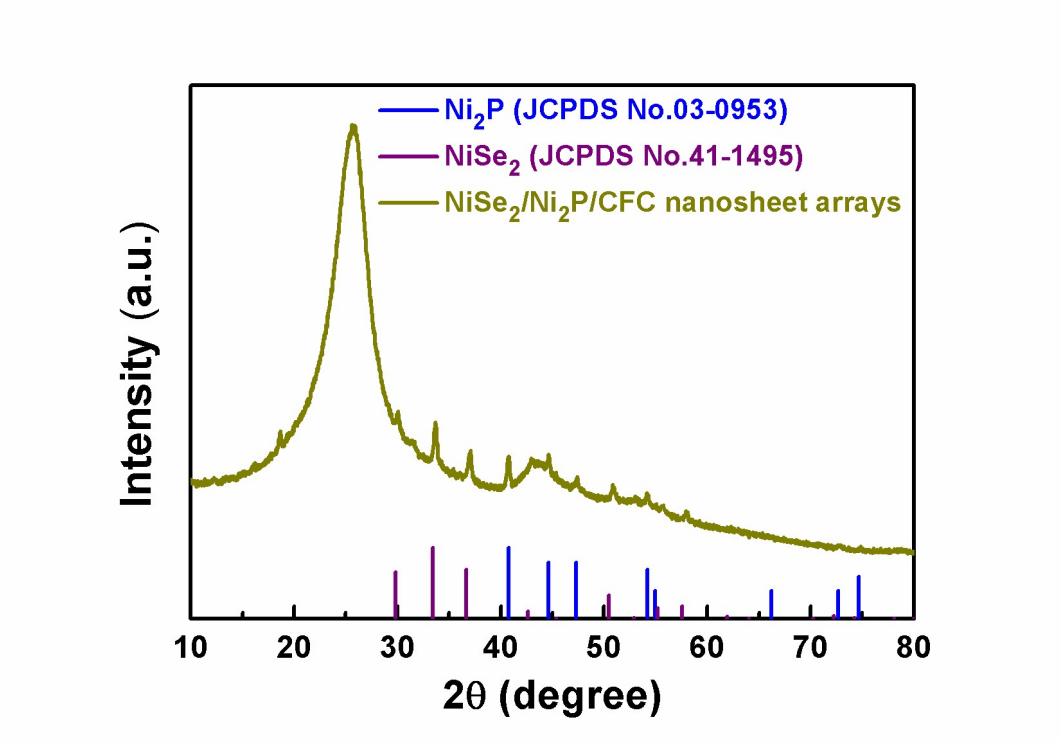

Fig. S5 XRD pattern of $Ni_2P/NiSe_2$/CFC heterogeneous nanosheet arrays.

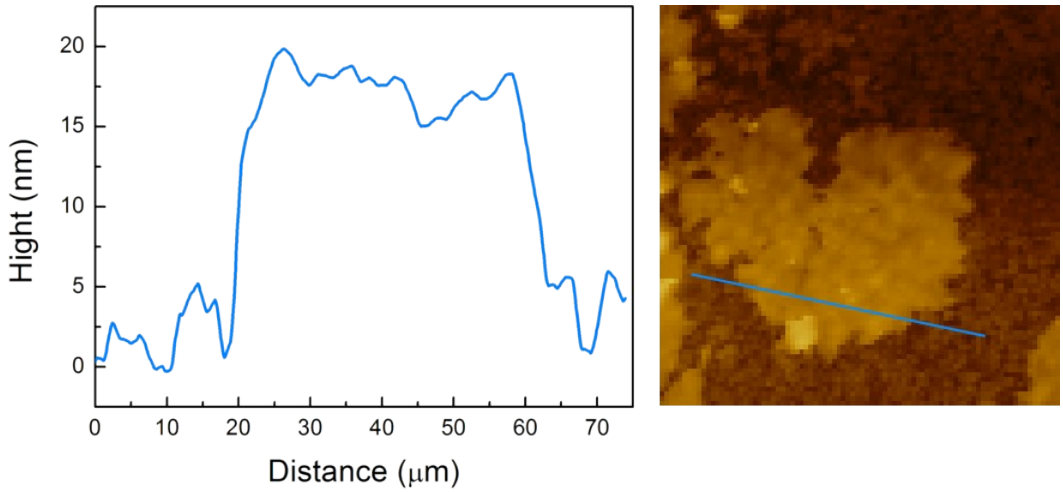

Fig. S6 AFM image and the corresponding height profiles of $Ni_2P/NiSe_2$ nanosheets for the thickness measurements.

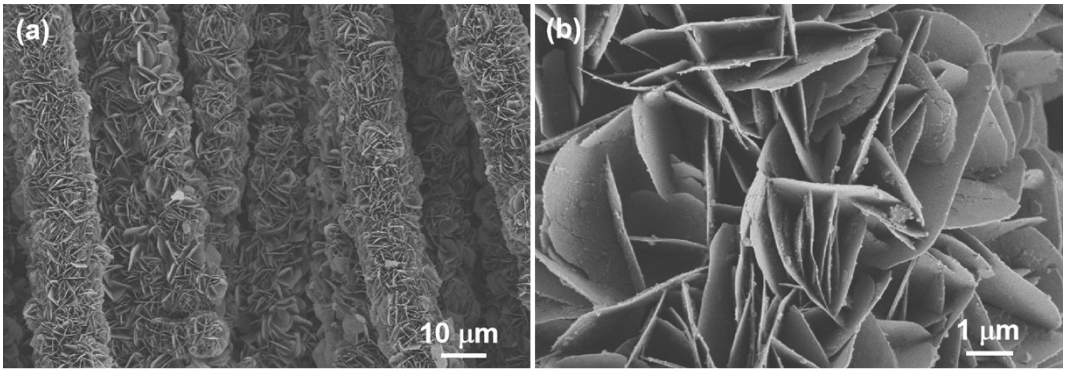

Fig. S7 (a) Low-magnification SEM image and (b) High-magnification SEM image of $NiSe_2$/CFC nanosheet arrays.

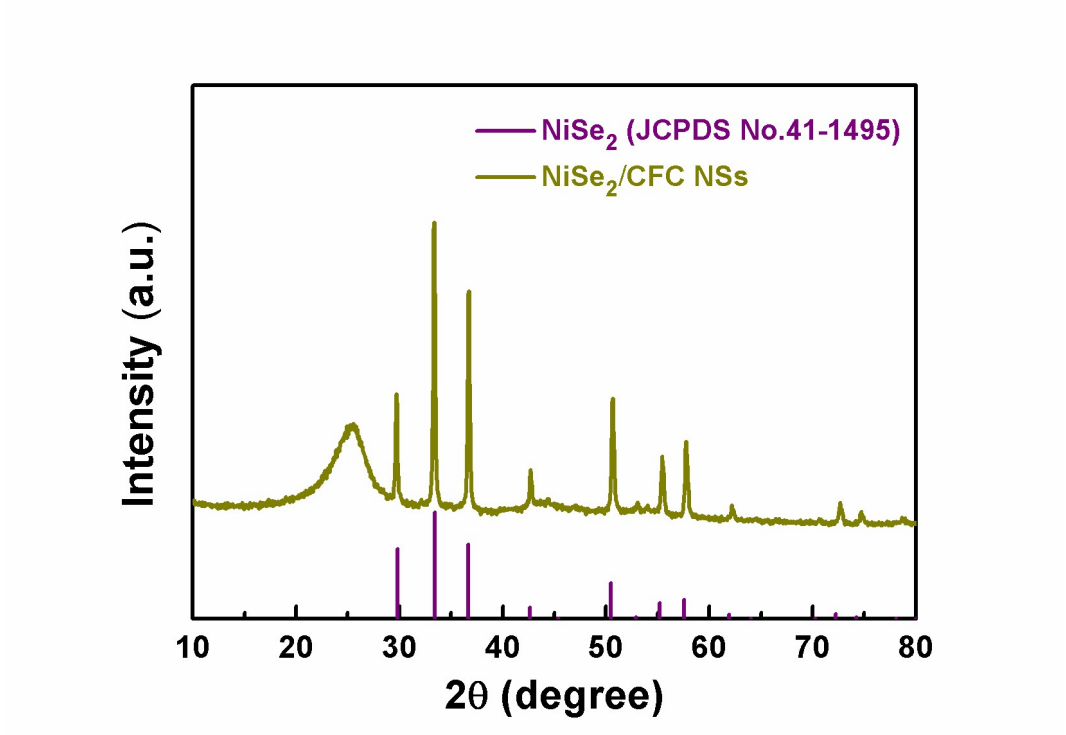

Fig. S8 XRD pattern of pristine $NiSe_2$/CFC nanosheet arrays.

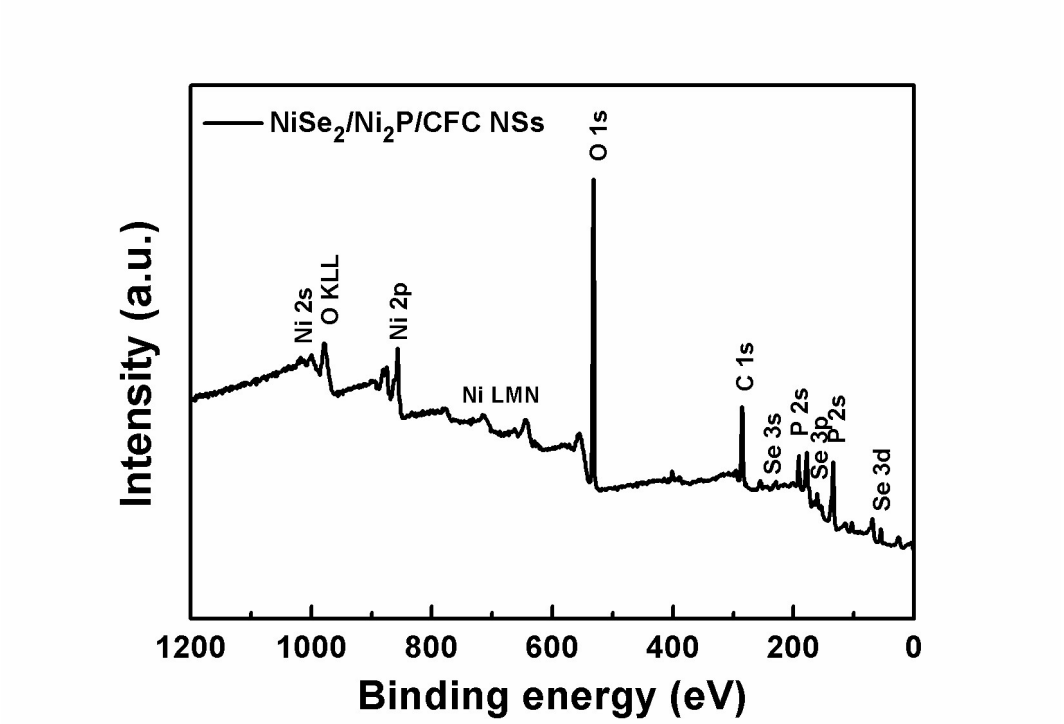

Fig. S9 The XPS survey spectrum of $Ni_2P/NiSe_2$/CFC heterogeneous nanosheet arrays.

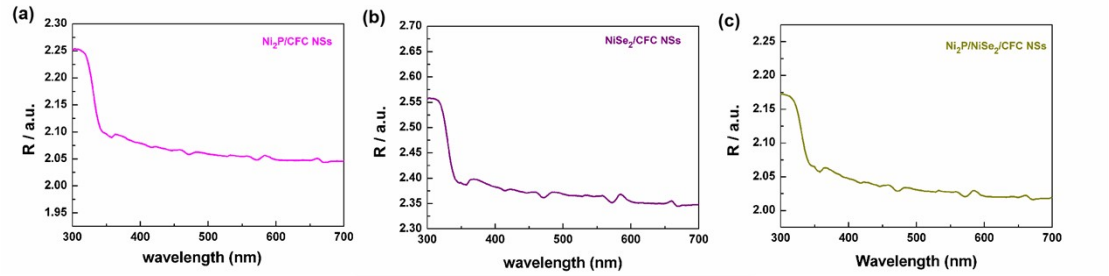

Fig. S10 UV-VIS diffuse reflectance spectra of (a) Ni_2P/CFC NSs, (b) $NiSe_2$/CFC NSs and $Ni_2P/NiSe_2$/CFC NSs at different scan rates in 1 M KOH.

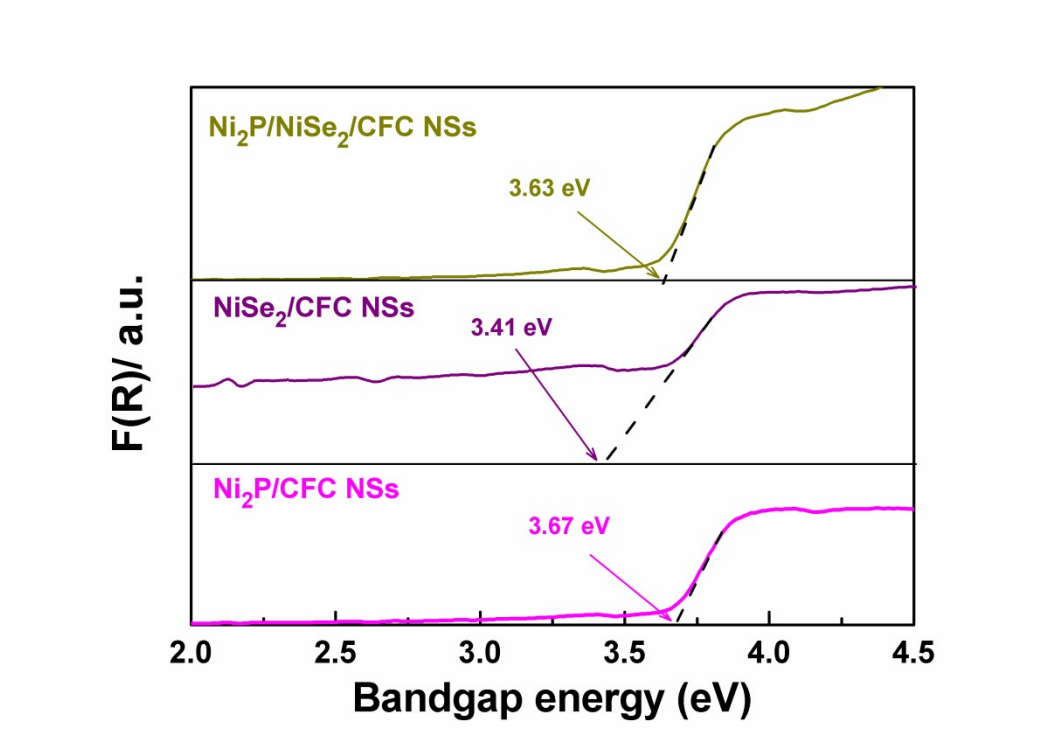

Fig. S11 UV/Vis spectra.

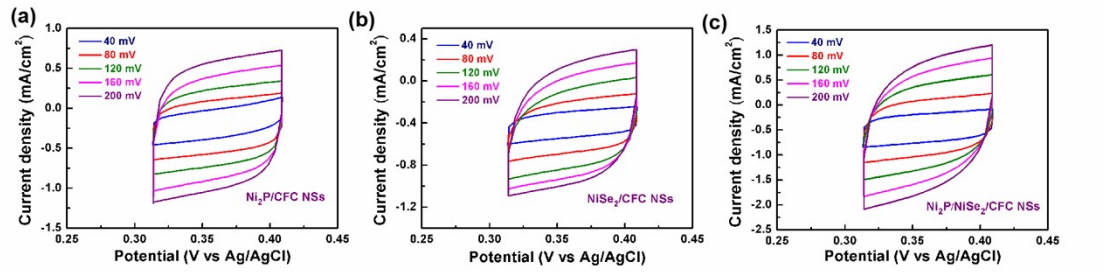

Fig. S12 Cyclic voltammograms of (a) Ni_2P/CFC NSs, (b) $NiSe_2$/CFC NSs and $Ni_2P/NiSe_2$/CFC NSs at different scan rates in 1 M KOH.

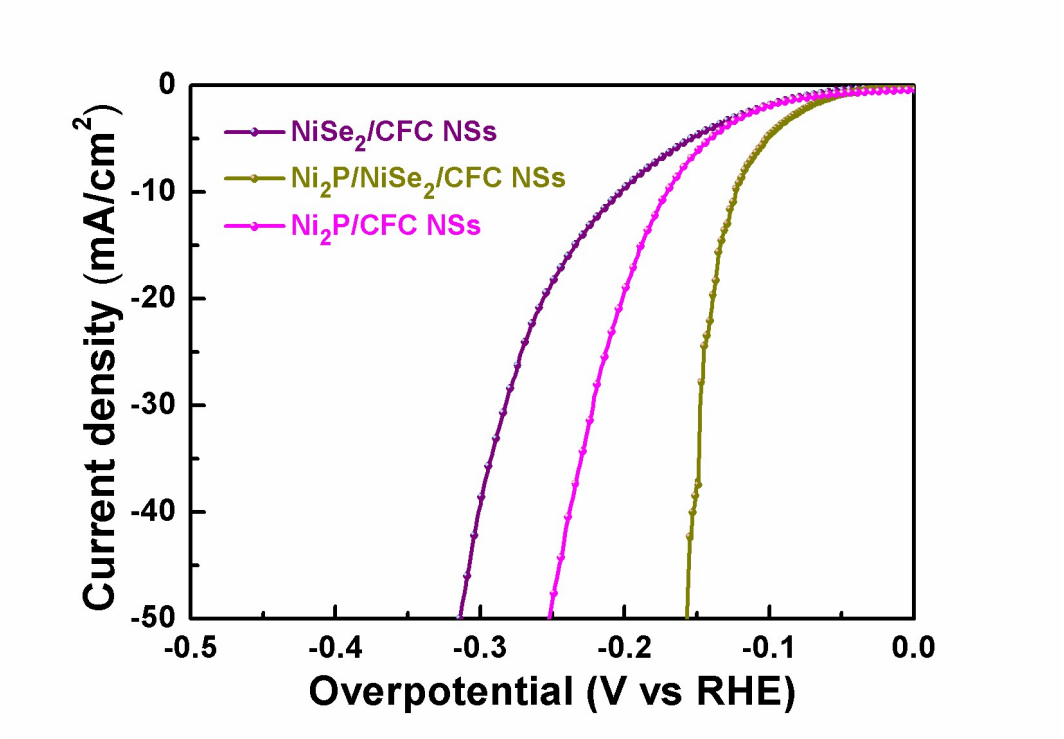

Fig. S13 HER polarization curves normalized by C_{dl}.

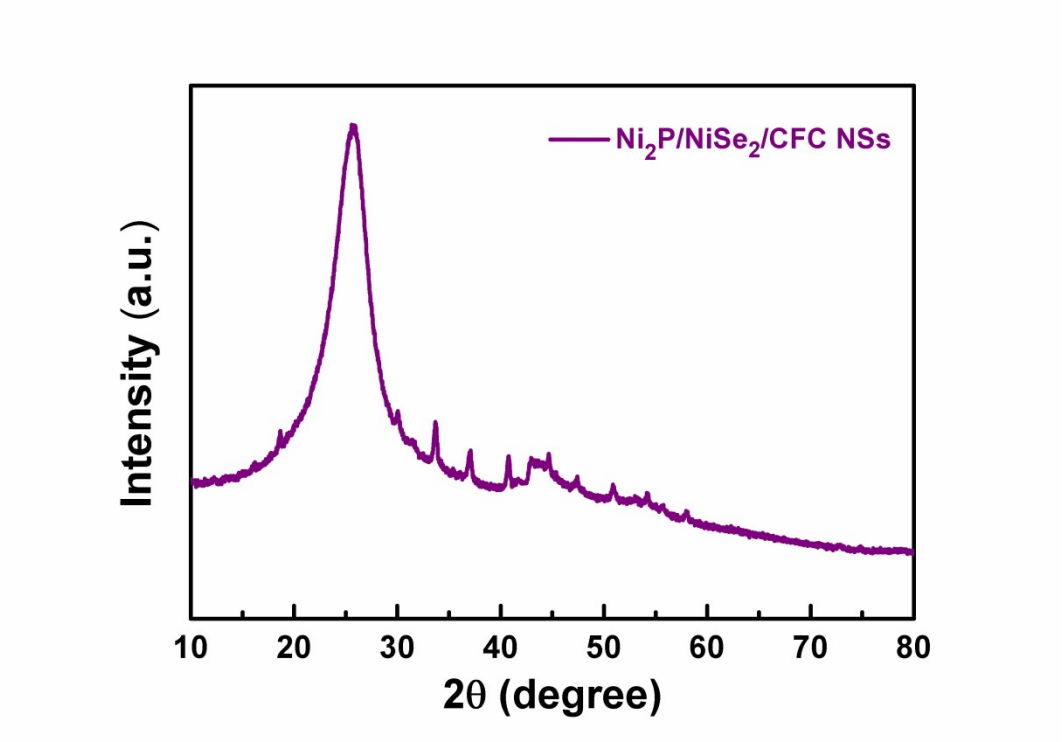

Fig. S14 XRD pattern of $Ni_2P/NiSe_2$/CFC NSs after durability test.

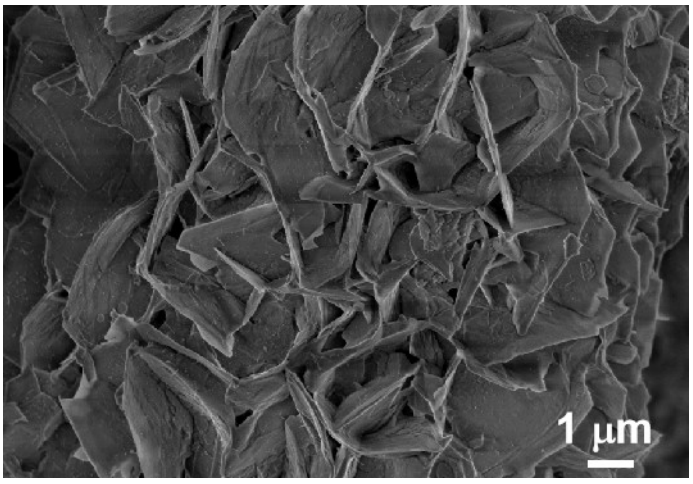

Fig. S15 SEM image of $Ni_2P/NiSe_2$/CFC NSs after durability test.

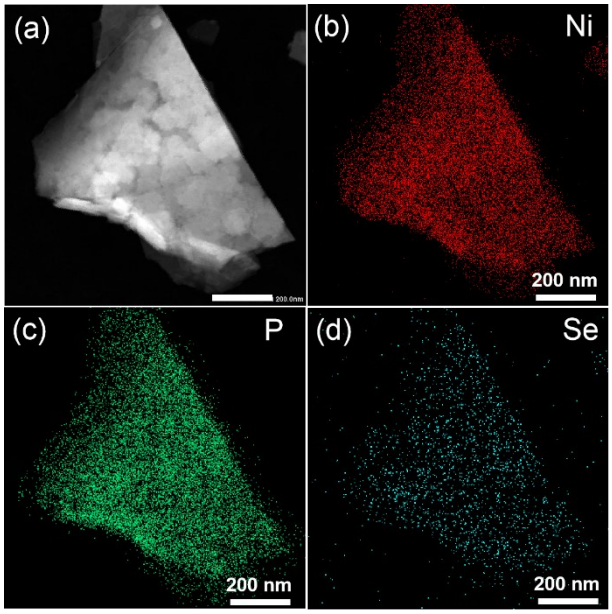

Fig. S16 Elemental mapping images of $Ni_2P/NiSe_2$/CFC NSs after OER durability test.

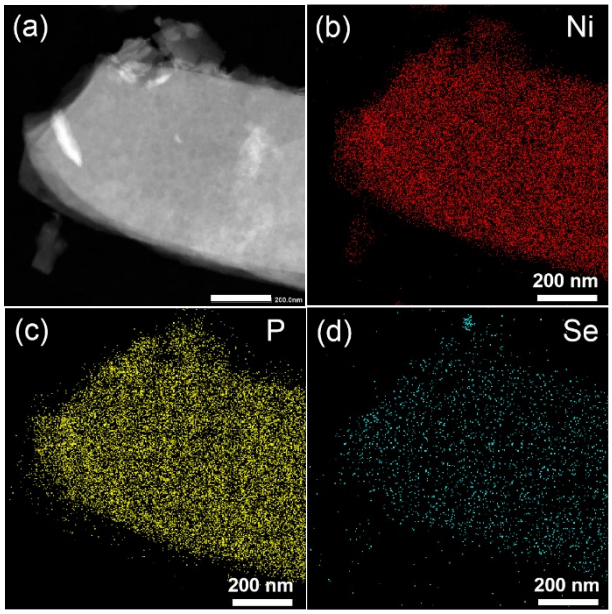

Fig. S17 Elemental mapping images of $Ni_2P/NiSe_2$/CFC NSs after uor durability test.

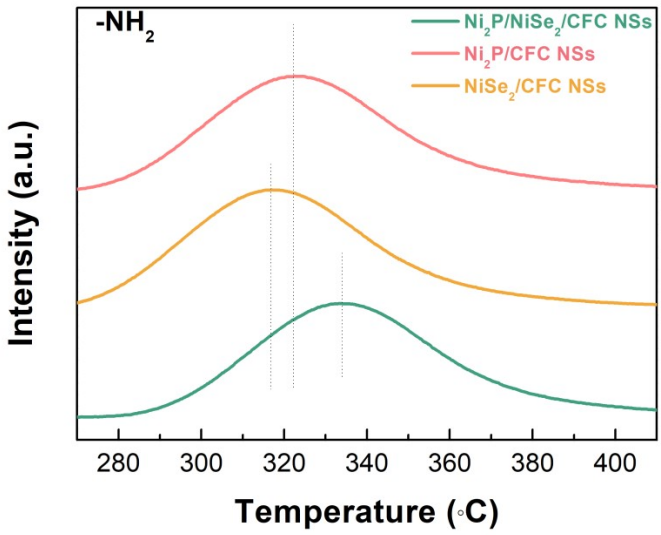

Fig. S18 TPD adsorption spectra of Ni_2P/CFC NSs, $NiSe_2$/CFC NSs, and $Ni_2P/NiSe_2$/CFC NSs in butylamine/He.

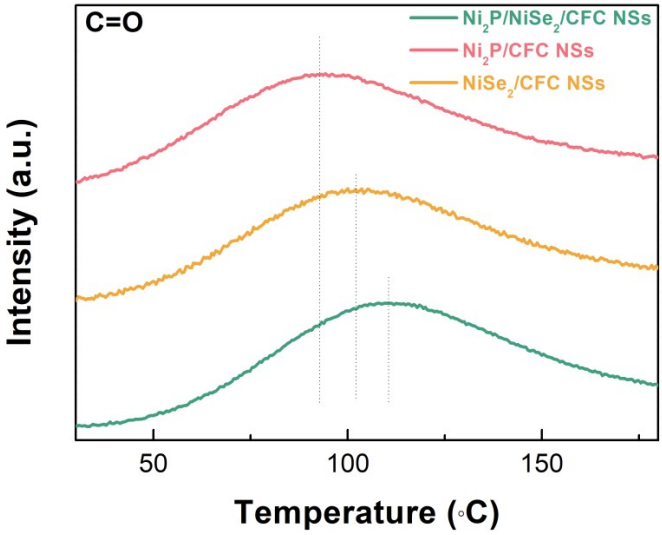

Fig. S19 TPD adsorption spectra of Ni_2P/CFC NSs, $NiSe_2$/CFC NSs, and $Ni_2P/NiSe_2$/CFC NSs in in CO atmospheres.

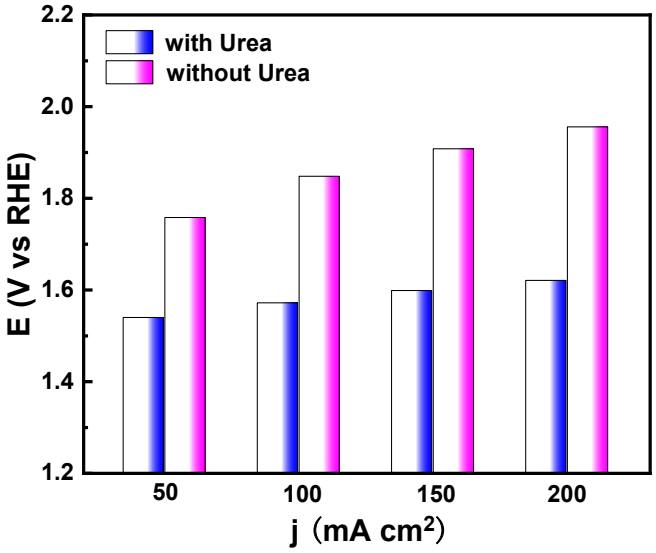

Fig. S20 Comparison for cell voltages of $Ni_2P/NiSe_2$/CFC NSs to deliver different current densities for water and urea electrolysis.

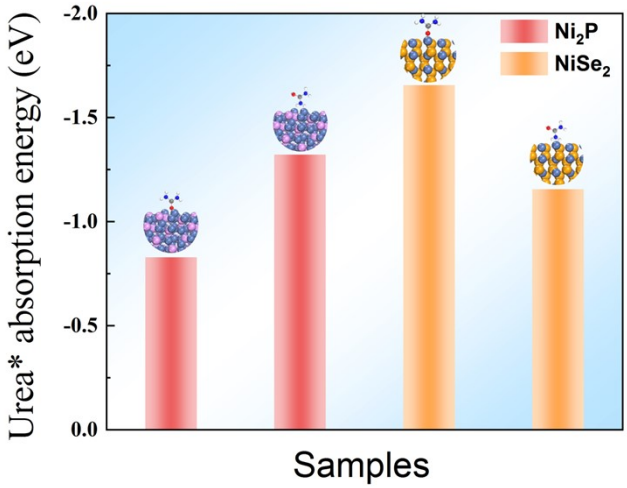

Fig. S21 Comparison of the adsorption energies of $-NH_2$ and CO groups in urea molecules adsorbed on Ni_2P and $NiSe_2$.

	0 h	12 h	24 h
pH	**13.96**	**13.91**	**13.88**

Table S1. Electrolyte pH changes with long-term stability test time.